

Surface Characterization of Laser Polished Indirect-SLS Parts

Jorge A. Ramos, David L. Bourell, Joseph J. Beaman
Laboratory for Freeform Fabrication
The University of Texas at Austin, Austin, Texas 78712

Abstract

Surface analysis was performed on laser polished indirect-SLS samples made from 420 stainless steel sintered powder - bronze infiltrated. The goal was to determine variations from the as-received condition in surface chemical composition, morphological structure, presence of contaminants as well as the formation of new phases. Comprehensive characterization of the laser polished surfaces was performed using scanning electron microscopy (SEM), energy dispersive spectrochemical analysis (EDS), x-ray diffraction analysis (XRD) and Vickers hardness. A large quantity of carbon (i.e. > 29 wt%) was present on the as-received surface mostly from the polymer binder present in the green part. Although surface-shallow-melting is the principal mechanism for the roughness reduction of the as-received surface, the chemical composition of the latter after processing changed to a higher carbon and oxygen content and a lower copper content. Additionally, clusters were formed periodically over the polished surface consisting of Fe, Cr, Si and Al oxides. The surface analysis demonstrated that the laser polished surfaces differ significantly more from a morphological rather than a microstructural perspective.

Introduction

The transition from Rapid Prototyping towards Rapid Manufacturing of functional parts requires adequate treatment of surface roughness to achieve R_a values below $1 \mu\text{m}$ ¹⁻⁵. Powder particle size, layer-wise building sequence, spreading of the powder and the resolution of the scanning/deposition system are factors that directly affect the final surface roughness on SLS processed parts⁴.

Samples provided by 3D Systems consisting of rectangular slabs made using LaserFormTM ST-100 material system were successfully laser polished. Results indicated that Laser Polishing is a fast and promising finishing technique for indirect-SLS metal parts and that up to a three-fold reduction in surface roughness could be achieved under certain circumstances⁶. However, the surface integrity of the laser polished surfaces has not been assessed until now. This includes the morphological, chemical and microstructural analysis of laser polished surfaces.

Schematics of Laser Polishing Process

A high power laser (either CO₂ or Nd:YAG) is used in continuous wave mode to laser polish the surface of the sample as illustrated in Figure 1. The focal spot size of the laser beam is within 0.35 mm. High speed galvanometer motor driven rotating mirrors provided a scanning speed of up to 750 mm/s and a traveling speed of up to 4.5 mm/s. The samples are located inside of a processing chamber that is evacuated to 200 mTorr and then back filled with an inert gas reducing atmosphere of 4.5% H₂+Ar.

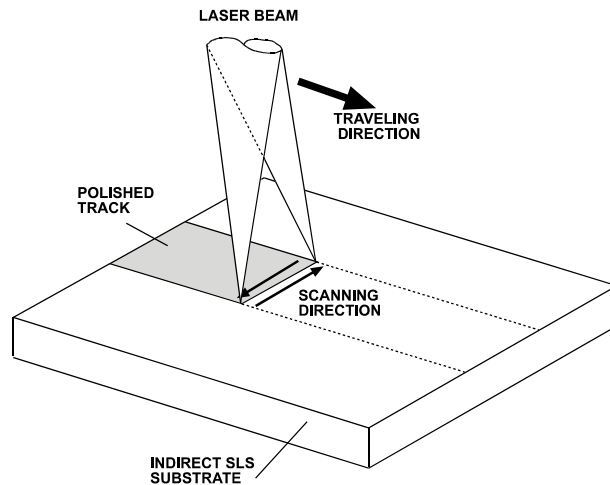


Figure 1. Schematic drawing of the laser polishing of a flat surface.

LaserFormTM ST-100 Surface Morphology

LaserForm ST-100 is a material system developed by 3D Systems (former DTM Corporation). It consists of 420 stainless steel powder containing a 2 wt.% polymer binder. A green pre-form is shaped out of this material using the standard SLS process. The pre-form is then completely covered with fine alumina and silica powder and placed inside a N₂ atmosphere furnace to burn off the binder and proceed with a 40 wt.% bronze (5 wt.% Sn) infiltration of the part. This material system is aimed towards tool making for the injection molding industry. The surface roughness of the as-received parts ranges from 9.0 to 2.4 μm depending on the SLS process parameters and stainless steel powder particle diameter. Generally, parts being manufactured using this material system require of post-machining and finishing operations.

Figure 2 shows the surface morphology of an as-received indirect-SLS sample having a surface roughness value between 7-9 μm. This surface consists of a close-packed arrangement of liquid phase sintered spherical particles of about 100 μm radius. On the other hand, Figure 3 shows the morphology of the surface of an as-received sample having a lower surface roughness between 2-5 μm. The surface appears covered with patches of solidified infiltration liquid with a spatial frequency of 50 μm. It is not

clear how those patches form; however, they appear to be the result of bead blasting or similar post-operation.

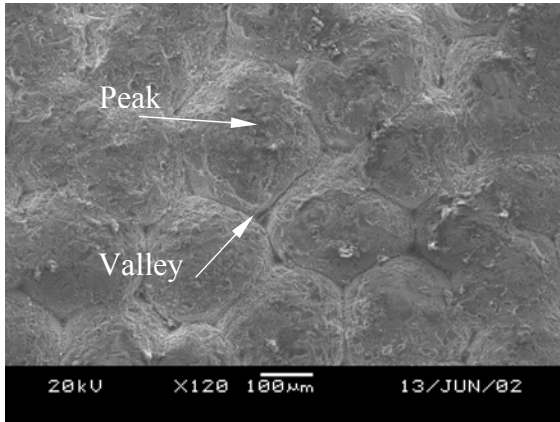


Figure 2. SEM image of the surface of indirect-SLS part having an $R_a = 7-9\mu\text{m}$, 120x.

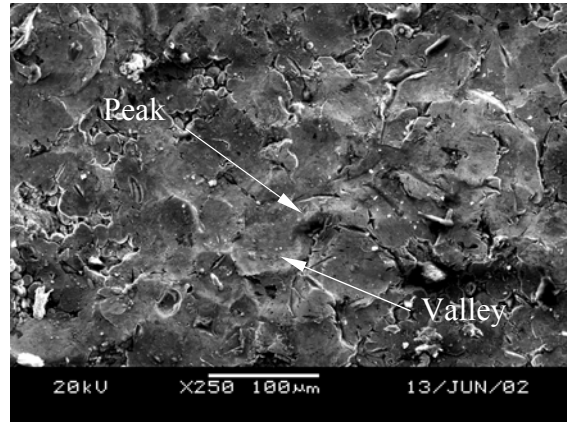


Figure 3. SEM image of the surface of indirect-SLS part having an $R_a = 2-5\mu\text{m}$, 250x.

Laser Polishing Mechanisms

In a previous research carried out by Ramos *et al*⁶ it was determined that two polishing mechanisms existed for the indirect-SLS metal part surfaces. These are:

- (i) Surface Shallow Melting (SSM) mechanism, where melting of surface apexes reduces the roughness R_a values by spreading of the melt over surface valleys driven by the pronounced curvature as illustrated in Figure 4. Capillary pressure is the driving mechanism minimizing curvature.
- (ii) Surface Over Melt (SOM) Mechanism, where excessive surface melting removes the original roughness but simultaneously induces capillary waves⁷ and surface ripples due to a surface tension gradient behind the laser front as explained in Figure 5. The material pulled away from the laser beam zone forms a wave that may freeze after solidification. The resulting surface roughness can increase due to these surface artefacts.

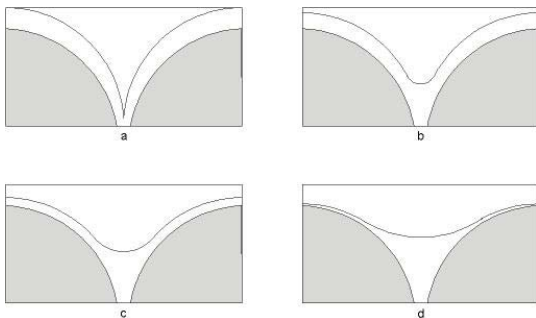


Figure 4. Schematic diagram of the SSM mechanism. Time sequence corresponds to $t_a > t_b > t_c > t_d$.

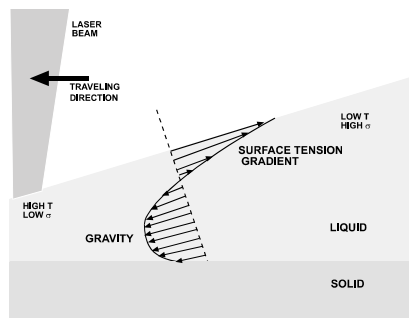


Figure 5. Schematic illustration of the rippling phenomenon encountered in the SOM mechanism.

Initial surface average roughness as well as laser power, scan speed and travelling speed determine which polishing mechanism operates. Figure 6 shows a laser polished track on an indirect-SLS surface achieved under the SSM mechanism. The surface roughness was reduced from 9.0 μm down to 3.2 μm . On the other hand, Figure 7 shows a laser polished track on an indirect-SLS surface achieved under the SOM mechanism. In this sample the surface roughness increased from 2.38 μm to 4.18 μm due to the excessive surface melting that induced a pattern of waves over the surface.

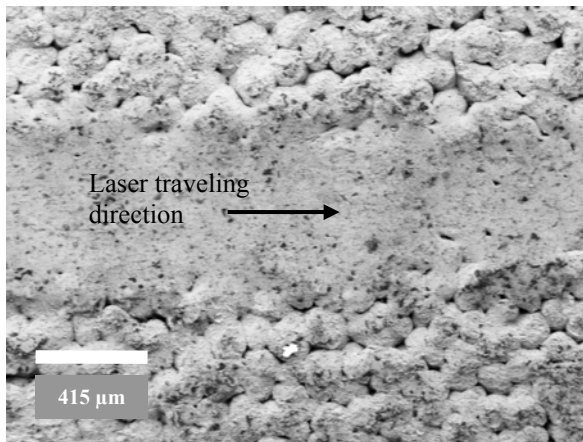


Figure 6. SEM image of a Nd:YAG laser polished track that has undergone Surface Shallow Melting, 60x. Adapted from Reference 6.



Figure 7. SEM image of a CO₂ laser polished track that has undergone Surface Over Melt, 50x. Adapted from Reference 6.

Results and Discussion

Figure 8 shows a laser polished track on a LaserForm ST-100 indirect-SLS surface achieved under the SSM mechanism. A 320 W CO₂ laser beam was used with a traveling speed of 4.5 mm/s. The average surface roughness was reduced from 2.38 μm down to 1.13 μm . Figure 9 shows a magnified laser polished area of the same sample, from which it can be observed that over the smoothed surface small clusters, 1 μm in radius, are distributed uniformly. Energy dispersive spectrochemical analysis (Figure 10 and Table 1) of the laser polished areas indicated that there is higher C and O content surface and lower Cu content than in the as-received. The high amount of C cannot be attributed to adsorbed CO₂ solely, but to the polymer binder present in the green part. During the burn-off stage of the sintering process the polymer forms carbonaceous compounds that are collected near the surface of the green part. From the EDS pattern shown in Figure 11 it can be seen that relative to the polished surface (Figure 10), the clusters contain less C but a higher amount of O and Cu as well as presence of Fe, Al, Cr and Si. It is likely that oxides of Fe, Cu and Cr were formed and that due to their low surface energy they were not wet by the molten copper and instead balled at the surface. Additionally, alumina and silica were trapped at the surface during the infiltration stage and emerged to the surface during the laser treatment.

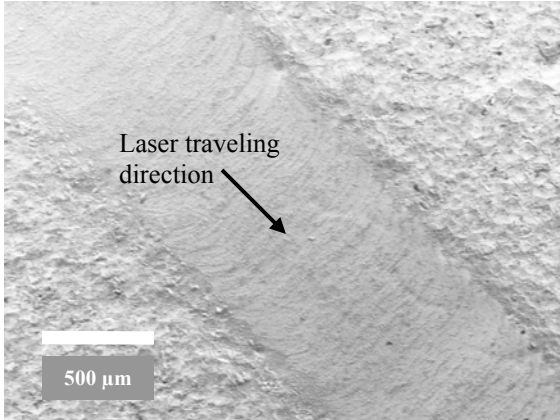


Figure 8. SEM image of SSM laser polishing mechanism, 50x. Adapted from Reference 6.

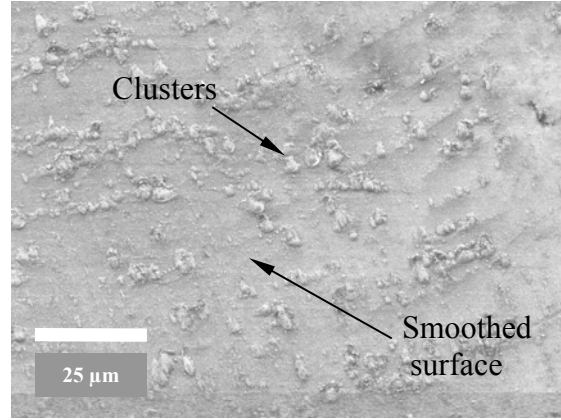


Figure 9. SEM image of the laser polished zone, 1000x.

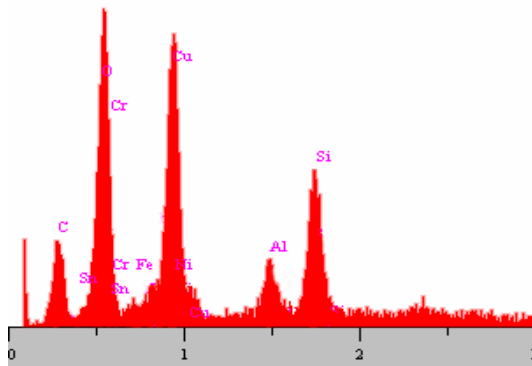


Figure 10. EDS pattern of a laser polished surface achieved under SSM mechanism.

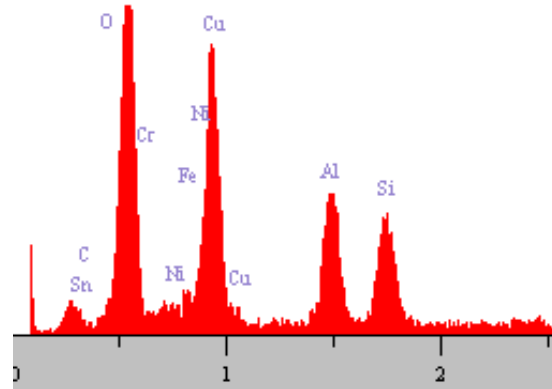


Figure 11. EDS pattern of clusters over laser polished surface achieved under SSM mechanism.

Figure 12 shows a laser polished track on a LaserForm ST-100 indirect-SLS surface achieved under the SOM mechanism. A 220 W CO₂ laser was used with a traveling speed of 4.5 mm/s. The average surface roughness increased from 2.38 μm down to 2.56 μm. Figure 13 shows a magnified laser polished area of the same sample. It can be observed that over the smoothed surface, long narrow ripples are distributed perpendicular to the laser traveling direction. EDS analysis (Figure 14 and Table 1) of the laser polished surface areas indicated that there is a lower C and O content than in the as-received surface, but a high Cu content. From Figure 15 and Table 1, it can be inferred that the ripples contained on average less C but a considerably higher O content as well as a strong presence of Al, Si and Cr compared to the smoothed areas. Again, this suggests that alumina and silica particles from the infiltration process are present in the ripples as well as some form of chromium oxide compound formed during the laser treatment.

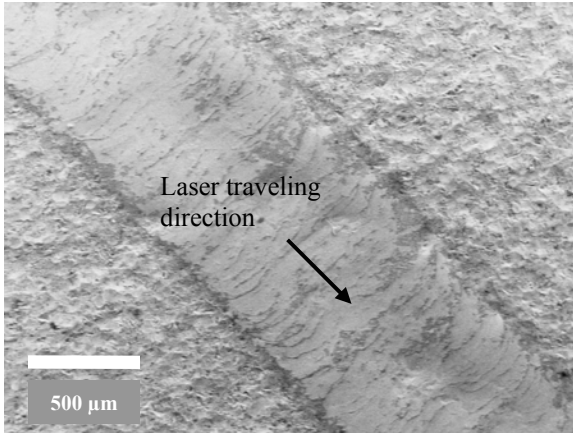


Figure 12. SEM image of SOM polishing mechanism, 50x. Adapted from Reference 6.

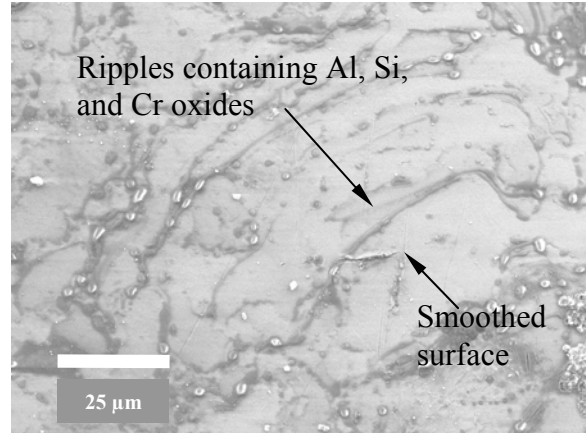


Figure 13. SEM image of the laser polished zone, 1000x.

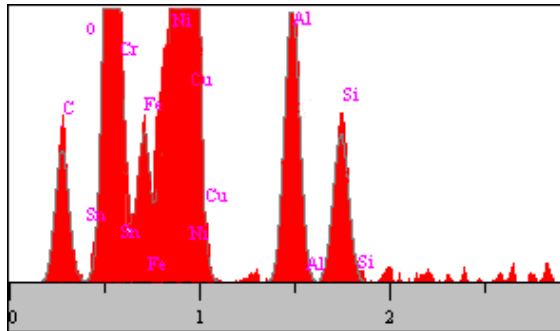


Figure 14. EDS pattern of laser polished surface under SOM mechanism.

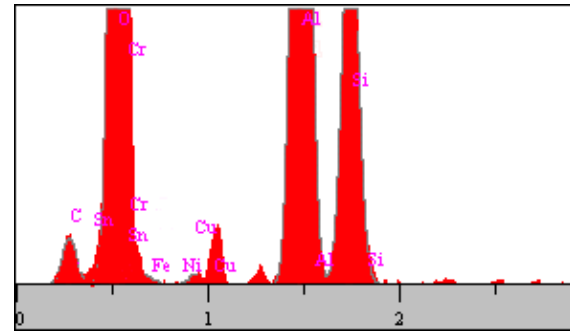


Figure 15. EDS pattern of ripple formation over laser polished surface under SOM mechanism.

Figure 16 shows a laser polished track on another LaserForm ST-100 indirect-SLS surface achieved under the SOM mechanism. The sample surface was treated with a CO₂ laser with power 220 W and traveling speed of 1.8 mm/s. The average surface roughness was increased in this case from 2.38 μm up to 4.18 μm. Multiple cracking of the treated surface can be observed in Figure 16. This may be associated with the difference in coefficient of thermal expansion between the bronze and the stainless steel as well as the high cooling rate experienced by the molten surface. Figure 17 shows a laser polished surface area of the same sample, where two distinct phases can be observed: a lighter phase and darker phase. The dark phase extends into elongated ripples. Moreover, fine white particles are observed over the dark phase areas. EDS analysis (Table 1) of the laser polished light phase areas indicates that C and O content experienced a slight decrease from the as-received condition while Cu content remained at the same level. Additionally, high Fe, Cr and Sn content are present in this phase. From the EDS analysis of the dark phase (Figure 18 and Table 1) a much higher O, Cr, Si and Sn content is exhibited than on the as-received surface while Cu content is almost negligible. The white particles over the dark phase areas consist of alumina particles (i.e., strong O and Al peaks seen in Figure 19) that in the as-received surface were hidden under the surface and after the laser polishing have emerged towards the surface.

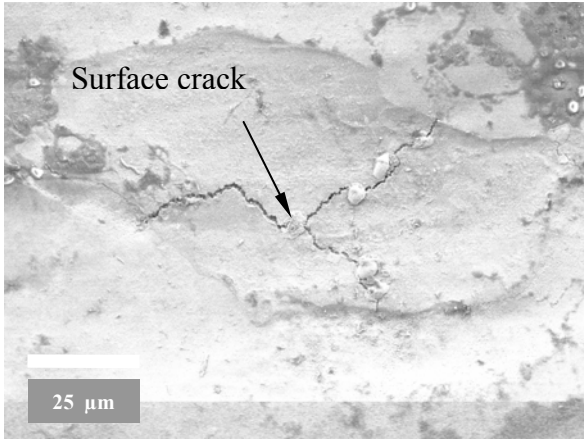


Figure 16. SEM of laser polished surface achieved under SOM mechanism, 1000x.

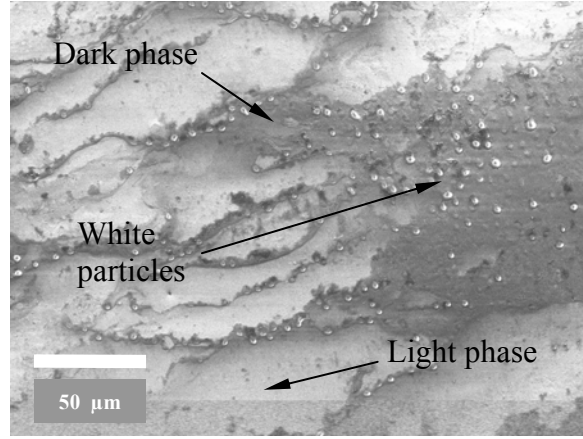


Figure 17. SEM of laser polished surface achieved under SOM mechanism, 500x.

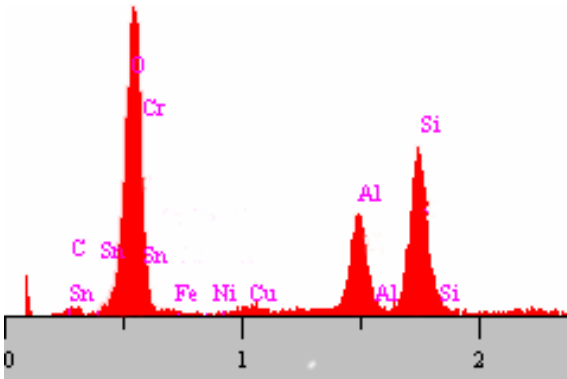


Figure 18. EDS pattern of laser polished surface achieved under SOM mechanism, dark phase.

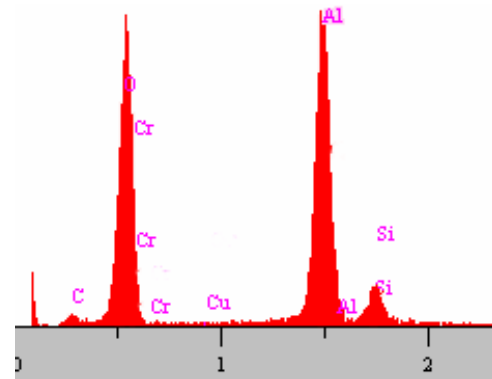


Figure 19. EDS pattern of a white particle over laser polished surface achieved under SOM mechanism.

Table 1. Quantitative chemical analysis (concentration weight %) of the surface of as-received and laser polished surface parts.

Element	As-received	SSM Polished surface Figure 9	Clusters Figure 9	SOM Polished surface Figure 13	Ripples Figure 13	SOM Polished surface light phase Figure 17	SOM Polished surface dark phase Figure 17	White particles Figure 17
C	28.99	43.44	28.17	13.16	10.53	23.02	14.41	17.56
O	14.79	17.37	25.56	11.02	47.22	11.95	36.56	47.21
Al	5.21	0.83	2.53	4.48	25.52	-----	5.47	23.28
Si	2.79	4.49	5.27	2.48	11.45	2.98	14.65	3.77
Cr	1.38	1.45	2.81	1.37	3.91	4.03	12.40	3.85
Fe	1.81	1.83	4.10	7.48	0.45	4.83	2.21	-----
Ni	1.98	1.78	2.08	0.14	-----	2.99	-----	-----
Cu	36.40	18.94	26.44	49.51	0.46	35.62	0.17	-----
Sn	6.60	9.09	2.26	10.34	0.44	14.04	11.90	-----

Figures 22 and 23 show the x-ray diffraction patterns of the indirect-SLS as-received surface and a laser polished surface achieved under the SSM mechanism. Figure 22 shows the presence of the expected Cu-Sn and Ni-Cr-Fe phases as well as for a Al-Si-Cr phase probably formed as a result of the infiltration process. For the laser polished surface there are no signs of amorphous phases as there is no broadening of the

peaks. It is known that the penetration of the x-rays can reach up to a couple mm from the surface, thus picking up most of the information from the unaltered bulk. However, a Cu_4O_3 phase was indexed associated with the molten copper contaminated with oxygen. Vickers hardness measurements were done on these two surfaces. The results are 193.6 HV for the as-received surface and 183.2 HV for the SSM laser polished surface. These results indicate that there are no small grains or amorphous microstructure formed during the solidification of the shallowly melted surface.

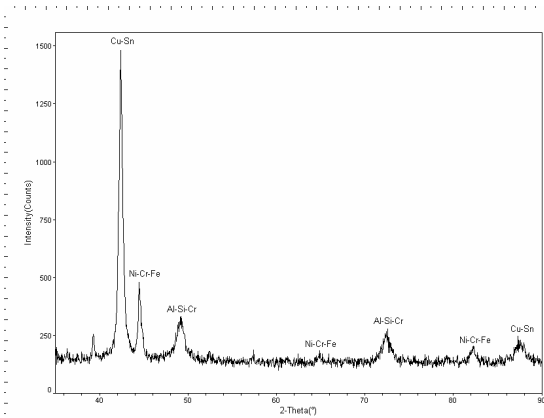


Figure 22. XRD pattern of as-received indirect-SLS surface.

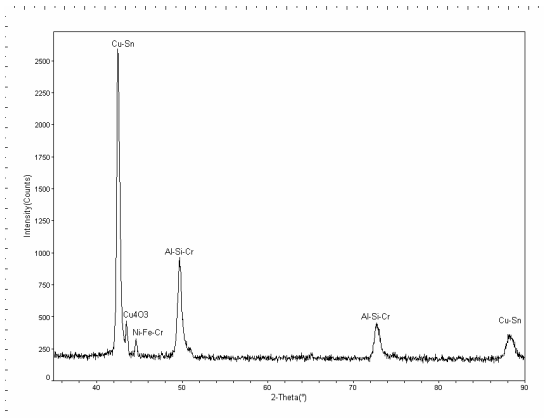


Figure 23. XRD pattern of laser polished surface achieved under SSM mechanism.

Conclusions

Carbon presence in the as-received surface, 29 wt.%, is oxidized during Surface Over Melt (SOM) laser polishing process down to 13-23 wt.%. On the other hand, for the Surface Shallow Melting (SSM) mechanism there is a significant carbon content increase, 44 wt.%, at the surface meaning that this element is being retained on the surface during under the SSM mechanism.

Surface chemical composition after SOM processing experienced higher iron, tin and copper content and lower carbon and oxygen content. Two phases are observed under the SEM, one lacking copper (dark colored phase) while the other phase lacks aluminium, but has more iron content (light colored phase). Ripples were formed periodically over the melted surface produced by the SOM mechanism. These consist of Al, Si, and possibly Cr oxides. These artefacts increase the roughness of the laser polished surface and could be removed using a laser ablative process. Some surface cracks are present near the edges of the polishing tracks.

After SSM processing more carbon, oxygen and silicon are observed together with a reduction in the aluminium and copper content. Small clusters consisting of iron, chromium, aluminium and silicon oxides are spread over the smoothed surface thus increasing its surface roughness. Presence of alumina and silica has its origin from the infiltration step.

XRD and hardness Vickers indicate that no significant microstructural changes are observed in the laser polished samples that experience the SSM mechanism compared to the as-received condition. The presence of a possible copper oxide phase was detected on the polished zones.

The laser polished surfaces differ significantly more from a morphological rather than a microstructural perspective.

References

1. J.J.Beaman, J.W.Barlow, D.L.Bourell, R.H.Crawford (1997): Solid Freeform Fabrication: A New Direction in Manufacturing. Kluwer Academic.
2. M. Burns (1993): Automated Fabrication: Improving Productivity in Manufacturing. Prentice-Hall.
3. J.A. McDonald, C.J. Ryall and D.I. Wimpenny (2001): Rapid Prototyping Casebook, Professional Engineering Publishing.
4. L. Lü, J. Fuh and Y.S. Wong (2001): Laser Induced Materials and Processes for Rapid Prototyping. Kluwer Academic.
5. J. Connolly, "Direct Rapid Manufacturing – Is it Possible?", Time Compression Technologies, May, pp. 46-47, 2001.
6. Ramos *et al*, "Surface Roughness Enhancement of Indirect-SLS Metal Parts by Laser Surface Polishing," (Paper presented at the 12th Solid Freeform Fabrication Symposium, Austin, Texas, August 2001).
7. V.S. Avanesov, M.A. Zuev, "Investigation of surface topography after melting by laser beam", SPIE Vol. 2713, 340-343.

Acknowledgments

The Laboratory for Freeform Fabrication gratefully acknowledges the support of the Office of Naval Research for funding the project "Surface Engineering for SFF Processes", Grant N^o: N00014-00-1-0334.

3D Systems (former DTM Corporation) provided LaserForm™ ST-100 samples for testing.